energies

MDPI

Article

Analytical Optimization of Vertical Closed-Loop Ground Source Heat Pump Systems

Konstantinos L. Katsifarakis and Yiannis N. Kontos *

Division of Hydraulics and Environmental Engineering, Department of Civil Engineering, Aristotle University of Thessaloniki, GR-54124 Thessaloniki, Greece; klkats@civil.auth.gr
* Correspondence: ykontos@civil.auth.gr; Tel.: +30-2310995708

Abstract: In this paper, we study the optimization of the operation of closed-loop ground source heat pump systems with any layout and any number n of vertical boreholes. Given the total required heat load, q_T, the goal is to maximize the rate of thermal gains from the ground or, equivalently, to minimize the disturbance of the ground temperature at the location of the boreholes. This is achieved by optimizing the distribution of q_T to the individual boreholes. We prove analytically that, at any time, the weighted temperature disturbance is minimal when the following condition holds: the temperature change is the same at the locations of all boreholes. Our proof is based on the analogy between heat transfer due to conduction and water flow through aquifers, and we make use of the results obtained for pumping cost minimization from systems of wells under transient groundwater flow conditions in infinite confined aquifers. Finally, we present a procedure to calculate the optimal distribution of the total heat load to the individual boreholes at any given time. The procedure entails the solution of a linear system of n equations and n unknowns, which is explained by means of two theoretical application examples. Accuracy of the results is also discussed.

Keywords: geothermal; ground source heat pump (GSHP); district heating; ground temperature change; optimization; analytical solution

Academic Editor: Mahmoud Bourouis

Received: 18 November 2024
Revised: 11 December 2024
Accepted: 1 January 2025
Published: 3 January 2025

Citation: Katsifarakis, K.L.; Kontos, Y.N. Analytical Optimization of Vertical Closed-Loop Ground Source Heat Pump Systems. *Energies* **2025**, *18*, 163. https://doi.org/10.3390/en18010163

1. Introduction

The transition from fossil fuels to renewable and soft energy sources is the only viable way to achieve human and environmental well-being. Still, it faces difficulties related mainly to high initial costs, competing land uses, and technical inefficiencies. Optimization at all stages (design, construction, and operation) can play a crucial role in supporting their market penetration, e.g., [1]. The proliferation of optimization techniques renders their application to the respective problems easier [2,3].

Low-enthalpy geothermal energy is a widely available renewable energy source that could contribute to the mitigation of global warming through the substitution of fossil fuels. Despite its renewability, its use should be properly designed in order to maintain its sustainability [4]. As its application for space heating is financially marginal in many cases, the further promotion of its use may require additional incentives, improved regulatory framework, certification schemes, and training activities [5], as well as proper guidelines [6]. The optimization of geothermal systems' crucial components or their overall designs can contribute substantially to their financial performance and, consequently, it can promote their penetration into fossil fuel-dominated markets (e.g., [7]). For this reason, it has attracted considerable research interest.

1.1. Literature Review

An indicative overview of the literature on the improvement of the overall design and/or operation of geothermal systems follows. The selected works are presented in chronological order.

Dickinson et al. [8] investigate combinations of ground source heat pump heating and cooling systems with other energy sources in order to reduce the installation costs while providing considerable economic and environmental savings. They use an incremental approach to demonstrate the importance of optimizing ground loop heat exchanger length. They conclude that compared to a peak-sized system, the capital cost of the optimum system is more than 60% lower while still providing more than 70% of the respective operational benefits.

Sayyaadi et al. [9] deal with the performance optimization of ground source heat pump (GSHP) systems, using (a) thermoeconomic criteria, (b) thermodynamic criteria, and (c) both criteria groups simultaneously. They use an evolutionary algorithm as an optimization tool. Their paper also includes a sensitivity analysis of optimal solutions to the interest rate, the electricity cost, and the number of operating hours in cooling mode.

De Paly et al. [10] examine closed-loop systems for district heating with many borehole heat exchangers. They use linear programming to minimize the maximum ground temperature change (maxΔT) at the borehole locations during the last time-step. Beck et al. [11] use metaheuristics to optimize borehole locations and linear programming to optimize their loads. Moreover, they include local groundwater flow, namely an additional advective energy supply, to the studied problem. Hecht-Méndez et al. [12] continue on the same path, using linear programming as the optimization tool. They mention that minimization of maxΔT results in leveling temperature distribution in the ground.

Carli et al. [13] investigate closed-loop heating and cooling systems with many borehole heat exchangers in a mild climate. They compare the typical split system for each flat with different combinations of district heating/cooling ground source heat pump systems with photovoltaics, boilers, or thermal solar collectors in areas with low and medium building densities. They conclude that (a) the financial benefits of centralized systems are larger in areas with medium building densities and (b) the combination of heat pumps with solar collectors results in the largest primary energy savings. Moreover, they discuss incentives to promote their use.

Retkowski and Thöming [14] aim to optimize the design of a closed-loop vertical GSHP system, including the depth and number of boreholes, the mass flow rate, and the type and number of heat pumps. They use the Generalized Reduced Gradient method and an evolutionary algorithm to achieve three optimization goals: (a) minimization of total annual cost (TAC), (b) the optimization of coefficient of performance (COP), which additionally serves as a measure of environmental performance, and (c) the minimization of TAC/COP, which leads to the calculation of Pareto optimal solutions. Using their method, the authors achieved a TAC reduction of more than 10% in case studies.

Ikeda et al. [15] propose a method to optimize energy systems that includes GSHP. It is based on the metaheuristic differential evolution algorithm, and its application is easy. According to the authors, it can lead to operating cost reduction in the order of 10%.

Farzanehkhameneh et al. [16] use genetic algorithms to optimize different features of the ground source heat exchangers of a residential building, such as the number of boreholes, their radius and length, the external pipe's radius, and the flow discharge inside the pipe.

Ma et al. [17] present an overview of works related to the optimization of GSHP systems. Their main conclusions are as follows: (a) More research works are aimed at the optimization of the design of GSHP systems, and fewer are aimed at the optimization

of their control. (b) Optimization, in particular, optimization based on multi-objective techniques, can result in the reduction of energy consumption. (c) Sensitivity analysis is useful in the formulation of optimization problems for GSHP systems in order to reduce the variables that should be optimized and, consequently, to reduce the complexity of these problems. (d) Applications of small and simplified problems have served to validate the majority of optimization results.

Moon et al. [18] use the particle swarm optimization algorithm to optimize the design of a typical closed-loop GSHP system (namely its ground heat exchanger, heat pump, and heat storage tank), aiming to reduce the required initial investment. The target buildings included a hospital, a school, and an apartment building. According to their results, the optimal design could reduce the total investment cost over 20 years by approximately 32% for hospital buildings, 29% for school buildings, and 23% for apartment buildings.

Cruz-Peragón et al. [19] use two objective functions to optimize both energy savings and the internal rate of return, namely an environmental and an economic parameter. The final selection is based on the Pareto optimality approach.

Cai et al. [20] evaluate the performance of a GSHP system over different periods of time. They find that results depend on the evaluation period and conclude that system optimization should be conducted over its entire life span. Bina et al. [21] study the long-term performance of GSHP systems in Japan. They analyze the performance degradation of these systems after 15 years of operation, and they relate it to soil temperature change.

Moreover, many papers deal with the optimization of heat pumps or other parts of mechanical equipment, e.g., Dagdas [22], Zhang et al. [23], while others concentrate on the mathematical modeling and/or the efficiency of ground heat exchangers, e.g., Florides et al. [24], Kim et al. [25], Luo et al. [26]. The improvement of heat pump construction has attracted research interest, as well (e.g., Kong et al. [27]).

Similar research has been conducted on open-loop systems, aiming to minimize groundwater temperature changes, among other goals. Park et al. [28] deal with the optimization of open-loop ground source heat pump systems with the following goals: (a) the maximization of heat pump performance coefficient (COP), (b) the minimization of operational cost (considered proportional to the amount of extracted or reinjected groundwater), and (c) the minimization of changes in groundwater level and temperature at wells and nearby areas. The first two are included in the objective function, while the third is expressed through a number of constraints, together with water injection temperature. The decision variables are groundwater extraction and injection rates. Genetic algorithms are used as optimization tools. The authors apply their simulation-optimization tool to a hypothetical and a real case in Korea. Park et al. [29] extend the previous work by including well locations in the optimization process. They use real-coded genetic algorithms as optimization tools, and they conclude that the well configuration for the GSHP system should be determined together with the well flow rates.

1.2. Research Objectives and Premises

In this paper, we study the optimization of the operation of vertical closed-loop ground source heat pump systems with many vertical boreholes. Our aim is to maximize the rate of thermal gains from the ground or, equivalently, to minimize the disturbance of the ground temperature at the locations of the boreholes by optimizing the distribution of the total required heat load q_T to the individual boreholes. In order to account for the importance of the contribution of each borehole j, we use the heat load q_j that it harnesses as the respective weight factor. We prove that, at any time, the weighted temperature disturbance is minimal when the following condition holds: the temperature change is the same at the locations of all boreholes.

Our proof is based on the analogy between heat transfer due to conduction and transient groundwater flow, which has been used by Theis [30] to establish the basic law of transient groundwater flow, as discussed in Section 3 of this paper. The analogy between aquifers and "aestifers" is explicitly discussed by Banks [31].

In our proof, we make use of the results obtained for pumping cost minimization from systems of wells in infinite confined aquifers. The optimization tool is analytical, and the validity of its results is restricted by the assumptions in the simulation process only. The obtained results are in line with works by different authors (e.g., [21]) relating the improvement of long-term GSHP systems' performance with the restriction of soil temperature changes. Finally, the optimization goal, namely, the minimization of soil temperature disturbance, is directly related to the increase in the heat pump's COP and the minimization of the GSHP system's environmental impact.

2. The Physical Problem and Its Mathematical Description

In the following section, we consider a closed-loop GSHP system working in the heating mode. The system has n boreholes, which have similar features. Adopting a two-dimensional approach, we use average temperatures and temperature changes along the system's boreholes. No restrictions on the layout of boreholes are imposed. We assume, however, that all boreholes have the same physical characteristics. First, we present the heat flow simulation model.

2.1. The Conductive Heat Flow Simulation Model

We consider two-dimensional conductive heat flow through the ground surrounding the GSHP system. This approach is compatible with the use of average ground temperature change along the boreholes. To simulate the effect of each vertical borehole on the temperature distribution, we consider an infinite line heat source of constant strength in an infinite homogeneous medium (Carslaw and Jaeger [32]). According to this model, which has been successfully used in connection with GSHP systems (e.g., [15]), the temperature change at any point p up to time t, due to one infinite line source j, is given as follows:

$$\Delta T_p = \frac{q_j}{4\pi L\lambda} \int_{\rho c \frac{r^2}{4\lambda t}}^{\infty} \frac{e^{-u}}{u} du \tag{1}$$

In Equation (1), q_j is the heat load of the heat source j [W], λ [W·m^{-1}·K^{-1}] is the thermal conductivity, L [m] is the borehole length, t [s] stands for time, and r [m] is the distance between the source j and point p, while c [J·kg^{-1}·K^{-1}] and ρ [kg·m^{-3}] are the specific heat capacity and the density of the ground, respectively. Following many previous works (e.g., [11,13]), we consider c and ρ as constants.

To simulate the overall temperature change, namely, the effect of the n boreholes, we use the superposition principle, which leads to the following equation:

$$\Delta T_m = \frac{1}{4\pi L\lambda} \sum_{j=1}^{n} q_j \int_{\rho c \frac{r_{ij}^2}{4\lambda t}}^{\infty} \frac{e^{-u}}{u} du \tag{2}$$

The use of this model allows for an analytical approach to the optimization problem, which does not introduce any additional approximation and facilitates general conclusions on the operation of GSHP systems.

2.2. Mathematical Formulation of the Optimization Problem

Our aim is to maximize the rate of thermal gains from the ground for a given configuration of a GSHP system and for a given total heat load q_T. This can be considered

as equivalent to the minimization of the ground temperature disturbance (drop) ΔT_j at the locations of the system's boreholes. At any time, the impact of ΔT_j at borehole j on the system's efficiency depends on the heat load q_j, required from that borehole. For this reason, the objective function GTD that should be minimized in order to maximize the rate of thermal gains from the ground can be stated in the following way:

$$GTD = \sum_1^n q_j \Delta T_j \tag{3}$$

In Equation (3), the heat loads q_j are the decision variables, while the terms ΔT_j should be calculated by simulating conductive heat flow through the ground around the boreholes. For this reason, the respective simulation model should be integrated in the optimization process.

The decision variables q_j should fulfill the following constraint set in the statement of the optimization problem:

$$\sum_{j=1}^n q_j = q_T \tag{4}$$

Moreover, since the GSHP system is working in the heating mode, the heat loads q_j should obtain non-negative values only, as follows:

$$q_j \geq 0, \quad 1 \leq j \leq n \tag{5}$$

Applying Equation (2) at the locations of the boreholes and inserting the results into Equation (3), we end up with the following form of the objective function:

$$GTD = \frac{1}{4\pi L\lambda} \sum_{j=1}^n q_j \sum_{i=1}^n q_i \int_{\frac{\rho c}{4\lambda t}}^{\infty} \frac{r_{ij}^2}{u} \frac{e^{-u}}{u} du \tag{6}$$

In Equation (6), r_{ij} is the distance between boreholes i and j, with heat loads q_i and q_j, respectively. Since the borehole length L is given and the soil properties are considered constant, the objective function can be reduced to the following equation:

$$GTD1 = \sum_{j=1}^n q_j \sum_{i=1}^n q_i \int_{\frac{\rho c}{4\lambda t}}^{\infty} \frac{r_{ij}^2}{u} \frac{e^{-u}}{u} du \tag{7}$$

Therefore, the final form of the optimization problem consists of the objective function described in Equation (7) and the constraints expressed in Equations (4) and (5). To solve the aforementioned optimization problem, we recall the similarity between the mathematical description of conductive heat flow through solids and that of water flow through aquifers.

3. Conductive Heat Flow Through Solids vs. Water Flow Through Aquifers

As early as 1935, Theis [30] observed the similarity between the mathematical description of conductive heat flow through solids and that of water flow through porous media and adapted the solution for heat conduction in solids produced previously by Carslaw [33] to transient groundwater flow problems. By matching hydraulic head level drawdowns (changes) with temperature changes and well flowrates with heat loads, Theis derived the following equation for transient hydraulic head level drawdown (simply called drawdown in the rest of this paper) in the case of one well pumping from an infinite confined aquifer:

$$s_m = \frac{Q_j}{4\pi T} \int_{\frac{Sr^2}{4Tt}}^{\infty} \frac{e^{-u}}{u} du \tag{8}$$

In Equation (8), s_m [m] is the drawdown at point m and at time t since the beginning of pumping, which is due to the pumping flow rate Q_j [m^3/s] from well j. T and S are the aquifer's transmissivity [m^2/s] and storativity [-], respectively.

In this paper, we follow the "opposite" approach. To solve the closed-loop GSHP system optimization problem described in the previous section, we use a solution for groundwater pumping cost minimization under transient flow conditions that was obtained by Katsifarakis et al. [34].

3.1. The Groundwater Pumping Cost Minimization Problem

In [34], the authors studied pumping cost minimization for any number and layout of wells under transient groundwater flow conditions in infinite confined and semi-infinite aquifers, to which the method of images applies. Moreover, they took into account the additional steady-state flow, independent of the examined system of wells, resulting in non-horizontal initial hydraulic head level distribution. For the case of infinite (and semi-infinite) aquifers without additional flow, it has been proven that, at any time, the instant pumping cost is minimal when drawdowns at all wells are equal. Similar results have been obtained in [35,36].

3.2. Similarity with the GSHP System Optimization Problem

The aforementioned groundwater pumping cost minimization problem is mathematically the same as that discussed in this paper if we substitute (a) the number of pumping wells with the number of boreholes of the closed-loop GSHP system, (b) the water level drawdowns s_j at the wells with the values ΔT_j of the soil temperature change at the locations of boreholes, and (c) the well flowrates Q_j with the borehole heat loads q_j. Moreover, both the objective functions and the constraints are similar if we substitute the total required well flow rate q_T with the total heat load q_T. The underlying physical similarities of the two problems include (a) the existence of a given number of concentrated loads with a given constant sum and (b) the impact pattern of any load on any location of the (heat or groundwater) flow field, which decreases with distance and increases with time.

In the following section, we briefly describe the procedure to minimize the objective function GTD1 given in Equation (7) under the constraints described in Equations (4) and (5).

4. The Optimization Procedure for the Closed-Loop GSHP System

As stated in Section 2, the objective function of the optimization problem, namely, Equation (7), is as follows:

$$GTD1 = \sum_{j=1}^{n} q_j \sum_{i=1}^{n} q_i \int_{\rho c \frac{r_{ij}^2}{4\lambda t}}^{\infty} \frac{e^{-u}}{u} du$$

The two constraints, namely, Equations (4) and (5), are as follows:

$$\sum_{j=1}^{n} q_j = q_T$$

$$q_j \geq 0, \quad 1 \leq j \leq n$$

To facilitate notation, we set the following equations:

$$v_{ijk} = c\rho \frac{r_{ij}^2}{4\lambda t_k} \tag{9}$$

and

$$W_{ijk} = \int_{v_{ijk}}^{\infty} \frac{e^{-u}}{u} du \tag{10}$$

We observe in (9) that v_{ijk} increases with distance r_{ij} and decreases with time t_k. We also observe that $v_{ijk} = v_{jik}$; consequently, $W_{ijk} = W_{jik}$. Moreover, the "exponential integral" W_{ijk}, which can be calculated using its serial expansion, decreases with increasing v_{ij} (namely with increasing r_{ij}) for any given time t_k, while it increases with time. It follows that W_{jjk}, corresponding to r_{jj}, namely, to the radius of borehole j, is larger than any W_{ijk} (with $i \neq j$).

Using the aforementioned notation, we can write the objective function, namely, Equation (7), in a more concise form, as follows:

$$GTD1 = \sum_{j=1}^{n} q_j \sum_{i=1}^{n} q_i W_{ijk} \tag{11}$$

Following the procedure described in [34,35], we calculate the first derivatives of GTD1 with respect to the decision variables, namely, the heat loads q_j. First, we note that they are not independent of each other since they are subject to the constraint (4). We can assume, without loss of generality, that the first $n-1$ heat loads are independent, while q_n depends upon the rest, as follows:

$$q_n = q_T - \sum_{i=1}^{n-1} q_i \tag{12}$$

Then, for any $m \in [1, n-1]$, we obtain the following equation:

$$\frac{\partial q_n}{\partial q_m} = -1 \tag{13}$$

Using Equation (13) we obtain the following equation for any $m \in [1, n-1]$:

$$\frac{\partial}{\partial q_m}\left(\sum_{i=1}^{n} q_i W_{ijk}\right) = W_{mjk} - W_{njk} \tag{14}$$

Using this result and the equality $W_{ijk} = W_{jik}$ to calculate the derivative of GTD1 with respect to q_m ($m \in [1, n-1]$), we obtain the following equation:

$$\frac{\partial GTD1}{\partial q_m} = 2\left(\sum_{i=1}^{n} q_i W_{imk} - \sum_{i=1}^{n} q_i W_{ink}\right) \tag{15}$$

Setting this derivative equal to zero, we obtain the following equation:

$$\frac{\partial GTD1}{\partial q_m} = 0 \Rightarrow \sum_{i=1}^{n} q_i W_{imk} = \sum_{i=1}^{n} q_i W_{ink} \Rightarrow \Delta T_m = \Delta T_n \tag{16}$$

Equation (16) holds for every $m \in [1, n-1]$. It follows, then, that (for any given t_k) a critical point of the objective function GTD1 occurs when the temperature changes at the locations of the boreholes are all equal.

Rearranging the terms in Equation (16), we obtain the following equation for every $m \in [1, n-1]$:

$$\sum_{i=1}^{n} q_i (W_{imk} - W_{ink}) = 0 \tag{17}$$

In the aforementioned sets of equations, the term W_{ijk} can be calculated from the respective field data (coordinates of the boreholes and soil features). The set of q_j values corresponding to the critical point can be found by solving a linear system of n equations and n unknowns. The first $n-1$ of them have the form of Equation (17), while the n-th

equation, which completes the system, is the constraint on the sum of the heat loads, namely, Equation (4).

This linear system has one solution only; namely, the objective function GDT1 has one critical point, P, only. To further check whether P corresponds to a minimum, and since GDT1 is twice continuously differentiable, we use its second derivatives, following the procedure described in [35]. Starting from Equation (15), we obtain the following equation:

$$\frac{\partial^2 GTD1}{\partial {q_m}^2} = W_{mmk} - W_{nmk} - W_{mnk} + W_{nnk} \quad (18)$$

As stated above, all W_{jjk} are larger than any W_{ijk} (with $i \neq j$) since they correspond to r_{jj}, namely, the radius of the respective borehole. So, the right-hand side of Equation (18) is positive; hence, the second derivative of GTD1 with respect to any q_m is positive. Consequently, the critical point P is either a minimum or a saddle point.

If it were a saddle point, GTD1 would exhibit a maximum at P, and it would be convex there along some "direction". According to the reasoning presented in [35], this is not possible. Hence, P is a local minimum; as it is the only critical point, P is the absolute minimum of GDT1.

After calculating the set of q_j values, which minimizes the ground temperature disturbance, the respective temperature change at the borehole locations can be calculated by applying Equation (2) to any of them. One should keep in mind, however, that the accuracy of the results is restricted by the simplifying assumptions in the heat flow simulation model mentioned in Section 2.1. The issue is further discussed in Section 5.3.

5. Application Procedure

The optimal distribution of the total heat load to the individual boreholes changes with time, following the increase in the "radius of influence" of each borehole and the respective temperature change. As long as the "radius of influence" is smaller than the smallest distance between the boreholes, namely, at the beginning of the operation of the GSHP system, the optimal choice is equal distribution of the total heat load. Then, the heat load distribution should be adopted from time to time, using the results obtained through the solution of the system of equations presented in the previous section as a guide.

To clarify the application of the proposed methodology, we use two hypothetical examples.

5.1. Application Example 1

In the first example, we adopt the borehole configuration discussed in [10,12]. It consists of 25 boreholes located at the vertices of a square lattice, as shown in Figure 1. The distances between successive boreholes are equal to 10 m. Moreover, we use the following values for the porous medium properties: thermal conductivity λ = 2.4 W·m^{-1}·K^{-1}, and volumetric heat capacity $C_V = c \cdot \rho$ = 2.6 × 10^6 J·m^{-3}·K^{-1}. Finally, we set the total heat load q_T = 100 in order to obtain the q_i values as percentages of q_T.

To calculate the time of first thermal interference between boreholes, we take into account that for $v_{ijk} \geq 7$, W_{ijk} tends toward 0. Then, setting v_{ijk} = 7 in Equation (9), we obtain the time of first interference, t_{k1}, as follows:

$$t_{k1} = C_V \frac{r_{ij}^2}{28\lambda} \quad (19)$$

For r = 10 m and the aforementioned values of λ and C_V, we have the following values:

$$t_{k1} = 3{,}869{,}047.6 \text{ s} = 1074.7 \text{ h}$$

According to this calculation, equal distribution of the heat load (namely setting each q_i equal to 4% of q_T) is the optimum choice for the first 1074 h. On the other hand, after 10,000 and 20,000 h of operation, the solution of the respective systems of 25 equations and 25 unknowns (as described in Section 4) leads to the heat load distribution of Tables 1 and 2, respectively. In these tables, q_i values appear as percentages of q_T.

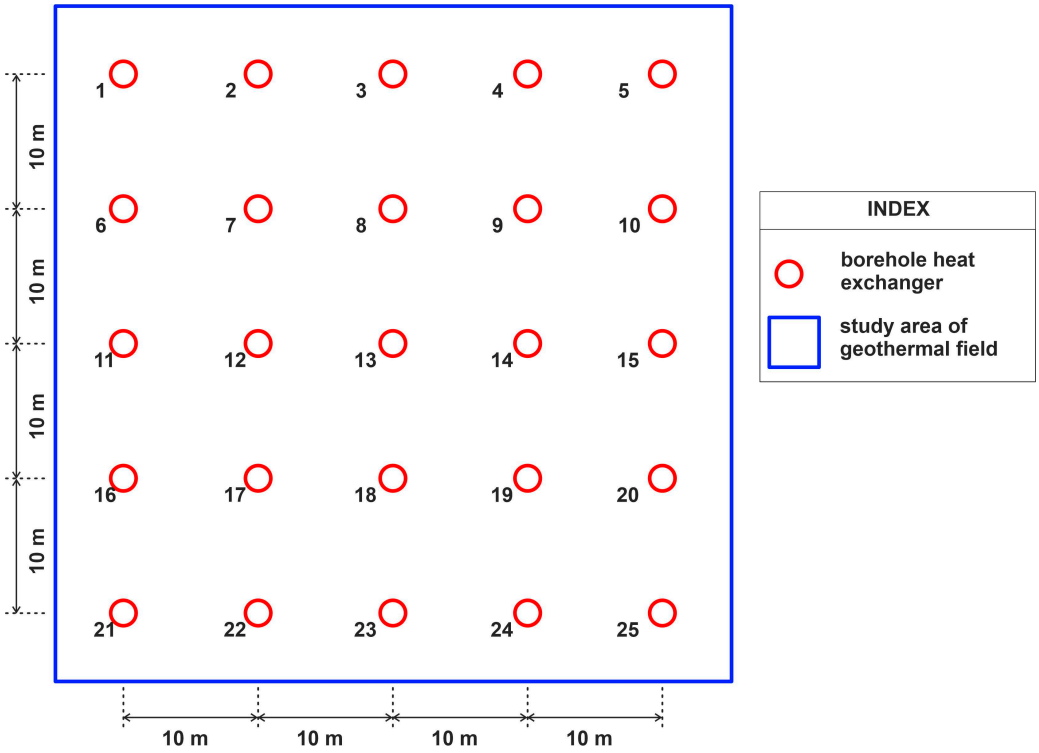

Figure 1. The borehole (BHE) configuration of the hypothetical GSHP system (adapted from [10]).

Table 1. Optimal heat loads q_i at the boreholes after 10,000 h of operation (shown as percentages of the total heat load q_T).

BHE Nr (*i*)	q_i (%) *	BHE Nr (*i*)	q_i (%) *
1	4.30	14	3.79
2	4.06	15	4.06
3	4.06	16	4.06
4	4.06	17	3.79
5	4.30	18	3.79
6	4.06	19	3.79
7	3.79	20	4.06
8	3.79	21	4.30
9	3.79	22	4.06
10	4.06	23	4.06
11	4.06	24	4.06
12	3.79	25	4.30
13	3.80		

* Red-white-green values indicate low-medium-high heat load values, respectively.

As shown in both tables, the heat flow distribution pattern is symmetrical. Moreover, the largest q_i values are found at boreholes 1, 5, 21, and 25, namely, at the corners of the borehole layout perimeter (shown in Figure 1), while the smallest are around the layout center. The ratios of the smallest to the largest q_i values are equal to 0.88 and 0.74 after 10,000 and 20,000 h of operation, respectively. It should be mentioned that the use of two decimal digits for the q_i values in Tables 1 and 2 does not imply that they have such a high

accuracy since the simulation model is approximate. However, the general pattern of the distribution of q_T to the individual boreholes can be considered accurate.

Table 2. Optimal heat loads q_i at the boreholes after 20,000 h of operation (shown as percentages of the total heat load q_T).

BHE Nr (*i*)	q_i (%) *	BHE Nr (*i*)	q_i (%) *
1	4.71	14	3.49
2	4.15	15	4.14
3	4.14	16	4.15
4	4.15	17	3.50
5	4.71	18	3. 49
6	4.15	19	3.50
7	3.50	20	4.15
8	3.49	21	4.71
9	3.50	22	4.15
10	4.15	23	4.14
11	4.14	24	4.15
12	3.49	25	4.71
13	3.47		

* Red-white-green values indicate low-medium-high heat load values, respectively.

5.2. Application Example 2

In many cases of practical interest, space restrictions, such as property limits or existing buildings, do not allow for symmetrical borehole configurations. For this reason, in the second application example, we consider the layout shown in Figure 2, which is presumably dictated by the available space. It consists of two borehole groups with 12 boreholes each. Their coordinates are presented in Table 3. Boreholes 1 to 12 belong to Group A, while the rest belong to Group B. Three sub-cases have been considered. In the first, only the boreholes of Group A are operating, while in the second, only those of Group B are operating. The total heat load is q_T for both sub-cases. In the third sub-case, all the boreholes are operating, and the total heat load is $2q_T$. We take into account the same soil features as in the previous example.

The optimal heat load distributions for the three sub-cases after 20,000 h of operation are shown in Table 4. The q_i values appear as percentages of q_T for Sub-cases 2.1 and 2.2 and $2q_T$ for Sub-case 2.3 to facilitate comparisons.

As shown in the second column of Table 4, the heat load distribution pattern of Sub-case 2.1 is quite similar to that of the first example; namely, it is symmetrical. The largest q_i values appear at the four corners of the borehole layout perimeter, and the smallest appear around the layout center.

The heat load distribution pattern of Sub-case 2.2, which is shown in the third column of Table 4, also has many similarities with that of the first example. It is symmetrical (as far as is allowed by the shape of the borehole layout); the smallest q_i values appear around the layout center, while the largest ones appear at the two vertices of the layout perimeter with the greatest distances from the rest of the boreholes (corresponding to the acute angles of the parallelogram).

The simultaneous operation of all boreholes (Sub-case 2.3) results in some changes in the optimal heat load distribution compared to Sub-cases 2.1 and 2.2. The overall contribution of the boreholes of Group A slightly decreases (by more than 1%), while that of Group B increases accordingly. The largest change appears in borehole 12, whose contribution decreased by 7.75%. This reduction is due to the proximity of borehole 12 to the Group B boreholes; the slightly larger distances between the boreholes of Group B can

explain the small overall increase in their contribution, which compensates for the small contribution decrease in the Group A boreholes.

As explained in the context of the first example, the use of two decimal digits for the q_i values summarized in Table 4 does not imply that they have such a high accuracy. This issue is further discussed in the following section.

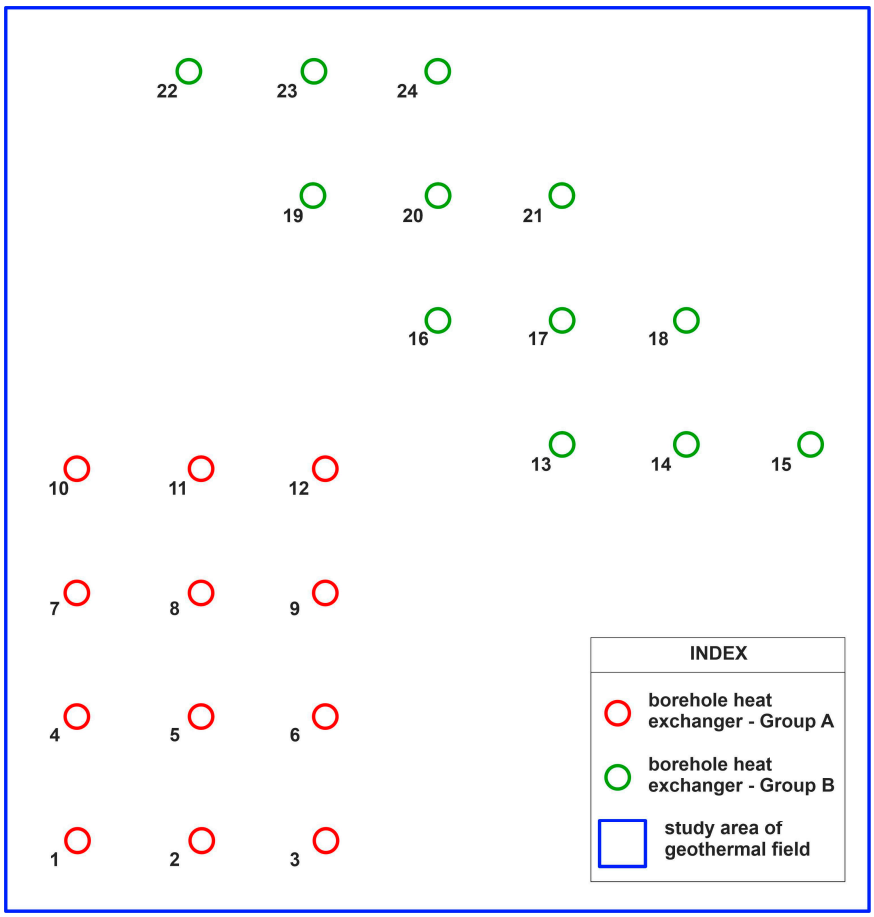

Figure 2. The borehole configuration of the hypothetical GSHP system of Example 2.

Table 3. Borehole coordinates of Example 2.

Group A		Group B	
i or BHE Nr	Coordinates x_i, y_i (m)	i or BHE Nr	Coordinates x_i, y_i (m)
1	0, 0	13	39, 32
2	10, 0	14	49, 32
3	20, 0	15	59, 32
4	0, 10	16	29, 42
5	10, 10	17	39, 42
6	20, 10	18	49, 42
7	0, 20	19	19, 52
8	10, 20	20	29, 52
9	20, 20	21	39, 52
10	0, 30	22	9, 62
11	10, 30	23	19, 62
12	20, 30	24	29, 62

Table 4. Optimal heat loads q_i for the 3 sub-cases of Example 2 at t = 20,000 h.

I or BHE Nr	Sub-Case 2.1 q_i (%)	Sub-Case 2.2 q_i (%)	Sub-Case 2.3 q_i (%)
1	9.29		9.16
2	8.20		8.09
3	9.29		9.16
4	8.17		8.05
5	6.89		6.79
6	8.17		8.05
7	8.17		8.06
8	6.89		6.80
9	8.17		7.98
10	9.29		9.15
11	8.20		8.01
12	9.29		8.57
13		8.58	8.64
14		8.10	8.33
15		9.68	9.96
16		8.27	8.11
17		7.08	7.25
18		8.29	8.53
19		8.29	8.42
20		7.08	7.27
21		8.27	8.52
22		9.68	9.95
23		8.10	8.34
24		8.58	8.83

5.3. Accuracy of the Results

The optimization procedure used in our paper is analytical; namely, it leads to the best solution to the set problem. Although the number of boreholes (decision variables) has a substantial impact on the computational load, it does not affect the accuracy of the results as long as available computational resources can handle large linear systems. Nevertheless, the accuracy of its results is restricted by the assumptions in the heat flow simulation model, which are mentioned in Section 2.1. A short discussion follows.

Our approach is based on modeling conductive heat flow only; namely, it ignores local groundwater flow, which can lead to a substantial increase in BHE performance, as shown in [37]. This assumption restricts the applicability of our approach only in cases of insignificant convective heat flow.

Ignoring temperature change with depth, which is implied by the use of a two-dimensional model for heat transfer, is functional to our model. If the boreholes have the same length, however, we believe that the influence of this simplification on the accuracy of the results is negligible.

The violation of the assumption of infinite homogeneous medium will distort the distribution of the total required heat load to the individual boreholes; however, it will not affect the basic distribution principle, namely, the equality of the resulting temperature disturbances, as long as the impact of any heat load on any location of the heat flow field decreases with distance and increases with time.

The assumption that the sources have constant total strength will definitely be violated in practical cases. Moreover, adjustment of heat load distribution cannot be continuous in praxis. We envisage that it will be performed in a stepwise manner. In the application examples of the previous sections, q_i values have been calculated as percentages of the total

required heat load q_T. Thus, the anticipated average q_T for the coming period can be used in each step to calculate the heat load distribution to the individual boreholes.

Finally, in practical applications, temperature measurements at the boreholes should be used to make adjustments whenever they are necessary. The respective measurement means and techniques are well documented [38]. The adjustments will include a reduction or increase in the heat load at boreholes, with temperature changes larger or smaller than the average, respectively.

6. Discussion and Conclusions

This paper deals with the optimization of the operation of a closed-loop GSHP system, which can have any number and layout of boreholes. Moreover, no restrictions on the total heat load requirement have been imposed.

The first issue of any optimization process is to define its goal. Many such goals regarding GSHP systems have been proposed in the literature. In this paper, we aimed to maximize the rate of thermal gains from the ground; this goal is equivalent to minimizing the effect of the time-dependent disturbance (drop) of ground temperature at the locations of the boreholes. Using the heat load q_j, harnessed by each borehole j, as the respective weight factor, we proved analytically that at any given time, the weighted temperature disturbance is minimal when the following condition holds: the temperature change is the same at the locations of all boreholes. In other words, the optimum is achieved when the disturbance caused by the operation of the closed-loop GSHP system is equal at all borehole locations; this coincides with equal heat load distribution (namely, the equal intensity of disturbance causes) in the early stage of a GSHP system operation only.

Our proof has been based on the analogy between heat transfer due to conduction and water flow through aquifers, and we have made use of results obtained for pumping cost minimization from systems of wells under transient groundwater flow conditions in infinite confined aquifers. The findings are similar, as well. As suggested for a number of groundwater pumping cost minimization problems, the optimum is achieved when the disturbance, namely, the hydraulic head drawdown, is the same at the locations of all wells. Thus, in both problems, the optimum does not correspond to the equality of the loads but to the equality of the resulting disturbances.

Moreover, we have presented a methodology for finding the time-dependent optimal heat load distribution by solving a linear system of n equations and n unknowns, where n is the number of boreholes of the GSHP system. This methodology allows for the optimal operation of a GSHP system.

Future research goals include (a) the extension of the optimization targets to GSHP systems installed in areas with substantial local groundwater flow and (b) the quantification of cost reduction resulting from the application of the proposed optimization process.

Author Contributions: Conceptualization, K.L.K.; methodology, K.L.K.; software, K.L.K.; validation, K.L.K.; investigation, K.L.K. and Y.N.K.; resources, K.L.K. and Y.N.K.; writing—original draft preparation, K.L.K. and Y.N.K.; writing—review and editing, K.L.K. and Y.N.K.; visualization, K.L.K. and Y.N.K.; supervision, K.L.K.; project administration, K.L.K. All authors have read and agreed to the published version of the manuscript.

Funding: This research did not receive any specific grant from funding agencies in the public, commercial, or not-for-profit sectors.

Data Availability Statement: The original contributions presented in this study are included in the article. Further inquiries can be directed to the corresponding author.

Conflicts of Interest: The authors declare no conflict of interest.

References

1. Baños, R.; Manzano-Agugliaro, F.; Montoya, F.G.; Gil, C.; Alcayde, A.; Gómez, J. Optimization methods applied to renewable and sustainable energy: A review. *Renew. Sustain. Energy Rev.* **2011**, *15*, 1753–1766. [CrossRef]
2. Pillay, T.L.; Saha, A.K. A Review of Metaheuristic Optimization Techniques for Effective Energy Conservation in Buildings. *Energies* **2024**, *17*, 1547. [CrossRef]
3. Thaeer Hammid, A.; Awad, O.I.; Sulaiman, M.H.; Gunasekaran, S.S.; Mostafa, S.A.; Manoj Kumar, N.; Khalaf, B.A.; Al-Jawhar, Y.A.; Abdulhasan, R.A. A Review of Optimization Algorithms in Solving Hydro Generation Scheduling Problems. *Energies* **2020**, *13*, 2787. [CrossRef]
4. Ungemach, P.; Papachristou, M.; Antics, M. Renewability versus sustainability. A reservoir management approach. In Proceedings of the European Geothermal Congress, Unterhaching, Germany, 30 May–1 June 2007. Paper 216.
5. Giambastiani, B.M.S.; Tinti, F.; Mendrinos, D.; Mastrocicco, M. Energy performance strategies for the large scale introduction of geothermal energy in residential and industrial buildings: The GEO.POWER project. *Energy Policy* **2014**, *65*, 315–322. [CrossRef]
6. Florides, G.; Kalogirou, S. Ground heat exchangers—A review of systems, models and applications. *Renew. Energy* **2007**, *32*, 2461–2478. [CrossRef]
7. Nguyen, A.; Tamasauskas, J.; Kegel, M. A method for fast economic optimization of large hybrid ground source heat pump systems. *Geothermics* **2022**, *104*, 102473. [CrossRef]
8. Dickinson, J.; Jackson, T.; Matthews, M.; Cripps, A. The economic and environmental optimisation of integrating ground source energy systems into buildings. *Energy* **2009**, *34*, 2215–2222. [CrossRef]
9. Sayyaadi, H.; Amlashi, E.H.; Amidpour, M. Multi-objective optimization of a vertical ground source heat pump using evolutionary algorithm. *Energy Convers. Manag.* **2009**, *50*, 2035–2046. [CrossRef]
10. de Paly, M.; Hecht-Méndez, J.; Beck, M.; Blum, P.; Zell, A.; Bayer, P. Optimization of energy extraction for closed shallow geothermal systems using linear programming. *Geothermics* **2012**, *43*, 57–65. [CrossRef]
11. Beck, M.; de Paly, M.; Hecht-Méndez, J.; Bayer, P.; Zell, A. Evaluation of the performance of evolutionary algorithms for optimization of low-enthalpy geothermal heating plants. In Proceedings of the 14th Annual Conference on Genetic and Evolutionary Computation, Philadelphia, PA, USA, 7–11 July 2012; pp. 1047–1054. [CrossRef]
12. Hecht-Méndez, J.; de Paly, M.; Beck, M.; Bayer, P. Optimization of energy extraction for vertical closed-loop geothermal systems considering groundwater flow. *Energy Convers. Manag.* **2013**, *66*, 1–10. [CrossRef]
13. De Carli, M.; Galgaro, A.; Pasqualetto, M.; Zarrella, A. Energetic and economic aspects of a heating and cooling district in a mild climate based on closed loop ground source heat pump. *Appl. Therm. Eng.* **2014**, *71*, 895–904. [CrossRef]
14. Retkowski, W.; Thöming, J. Thermoeconomic optimization of vertical ground-source heat pump systems through nonlinear integer programming. *Appl. Energy* **2014**, *114*, 492–503. [CrossRef]
15. Ikeda, S.; Choi, W.; Ooka, R. Optimization method for multiple heat source operation including ground source heat pump considering dynamic variation in ground temperature. *Appl. Energy* **2017**, *193*, 466–478. [CrossRef]
16. Farzanehkhameneh, P.; Soltani, M.; Moradi Kashkooli, F.; Ziabasharhagh, M. Optimization and energy-economic assessment of a geothermal heat pump system. *Renew. Sustain. Energy Rev.* **2020**, *133*, 110282. [CrossRef]
17. Ma, Z.; Xia, L.; Gong, X.; Kokogiannakis, G.; Wang, S.; Zhou, X. Recent advances and development in optimal design and control of ground source heat pump systems. *Renew. Sustain. Energy Rev.* **2020**, *131*, 110001. [CrossRef]
18. Moon, H.; Jeon, J.-Y.; Nam, Y. Development of Optimal Design Method for Ground-Source Heat-Pump System Using Particle Swarm Optimization. *Energies* **2020**, *13*, 4850. [CrossRef]
19. Cruz-Peragón, F.; Gómez-de la Cruz, F.J.; Palomar-Carnicero, J.M.; López-García, R. Optimal design of a hybrid ground source heat pump for an official building with thermal load imbalance and limited space for the ground heat exchanger. *Renew. Energy* **2022**, *195*, 381–394. [CrossRef]
20. Cai, W.; Wang, F.; Shuang Chen, S.; Chen, C.; Zhang, Y.; Kolditz, O.; Shao, H. Importance of long-term ground-loop temperature variation in performance optimization of Ground Source Heat Pump system. *Appl. Therm. Eng.* **2022**, *204*, 117945. [CrossRef]
21. Mohammadzadeh Bina, S.; Fujii, H.; Kosukegawa, H.; Inagaki, F. A predictive model of long-term performance assessment of Ground Source Heat Pump (GSHP) systems in Japanese regions. *Geothermics* **2024**, *119*, 102955. [CrossRef]
22. Dagdas, A. Heat exchanger optimization for geothermal district heating systems: A fuel saving approach. *Renew. Energy* **2007**, *32*, 1020–1032. [CrossRef]
23. Zhang, H.; Hao, S.; Wen, M.; Bai, X.; Liu, L.; Zhang, P. Optimization of Ground Source Heat Pump System Based on TRNSYS in Hot Summer and Cold Winter Region. *Buildings* **2024**, *14*, 2764. [CrossRef]
24. Florides, G.; Theofanous, E.; Iosif-Stylianou, I.; Tassou, S.; Christodoulides, P.; Zomeni, Z.; Tsiolakis, E.; Kalogirou, S.; Messaritis, V.; Pouloupatis, P.; et al. Modeling and assessment of the efficiency of horizontal and vertical ground heat exchangers. *Energy* **2013**, *58*, 655–663. [CrossRef]
25. Kim, J.; Hong, T.; Chae, M.; Koo, C.; Jeong, J. An Environmental and Economic Assessment for Selecting the Optimal Ground Heat Exchanger by Considering the Entering Water Temperature. *Energies* **2015**, *8*, 7752–7776. [CrossRef]

26. Luo, J.; Rohn, J.; Bayer, M.; Priess, A. Thermal Efficiency Comparison of Borehole Heat Exchangers with Different Drillhole Diameters. *Energies* **2013**, *6*, 4187–4206. [CrossRef]
27. Kong, D.; Wan, R.; Chen, J.; Kang, J.; Jiao, X. Effect of gradation on the thermal conductivities of backfill materials of ground source heat pump based on loess and iron tailings. *Appl. Therm. Eng.* **2020**, *180*, 115814. [CrossRef]
28. Park, D.K.; Kaown, D.; Lee, K.-K. Development of a simulation-optimization model for sustainable operation of groundwater heat pump system. *Renew. Energy* **2020**, *145*, 585–595. [CrossRef]
29. Park, D.; Lee, E.; Kaown, D.; Lee, S.-S.; Lee, K.-K. Determination of optimal well locations and pumping/injection rates for groundwater heat pump system. *Geothermics* **2021**, *92*, 102050. [CrossRef]
30. Theis, C.V. The relation between lowering of the piezometric surface and the rate and duration of discharge of a well using ground water storage. *Eos Trans. Am. Geophys. Union* **1935**, *16*, 519–524. [CrossRef]
31. Banks, D. *An Introduction to Thermogeology: Ground Source Heating and Cooling*; John Wiley & Sons, Ltd.: Hoboken, NJ, USA, 2012. [CrossRef]
32. Carslaw, H.S.; Jaeger, J.C. *Conduction of Heat in Solids*; Oxford University Press: New York, NY, USA, 1959; 522p, ISBN 9780198533689.
33. Carslaw, H.S. *Introduction to the Mathematical Theory of the Conduction of Heat in Solids*; Macmillan and Co., Ltd.: London, UK, 1921.
34. Katsifarakis, K.L.; Nikoletos, I.A.; Stavridis, C. Minimization of Transient Groundwater Pumping Cost—Analytical and Practical Solutions. *Water Resour. Manag.* **2018**, *32*, 1053–1069. [CrossRef]
35. Katsifarakis, K.L. Groundwater Pumping Cost Minimization—An Analytical Approach. *Water Resour. Manag.* **2008**, *22*, 1089–1099. [CrossRef]
36. Ahlfeld, D.P.; Laverty, M.M. Analytical solutions for minimization of energy use for groundwater pumping. *Water Resour. Res.* **2011**, *47*, W06508. [CrossRef]
37. Antelmi, M.; Turrin, F.; Zille, A.; Fedrizzi, R. A New Type in TRNSYS 18 for Simulation of Borehole Heat Exchangers Affected by Different Groundwater Flow Velocities. *Energies* **2023**, *16*, 1288. [CrossRef]
38. Bertermann, D.; Suft, O. Determination of the Temperature Development in a Borehole Heat Exchanger Field Using Distributed Temperature Sensing. *Energies* **2024**, *17*, 4697. [CrossRef]